

Linear cosmological perturbations in Scalar-tensor-vector gravity

Sara Jamali^a **Mahmood Roshan**^{a,b} and **Luca Amendola**^c

^aDepartment of Physics, Ferdowsi University of Mashhad, P.O. Box 1436, Mashhad, Iran

^bSchool of Astronomy, Institute for Research in Fundamental Sciences (IPM), P.O. Box 19395-5531, Tehran, Iran

^cInstitute for Theoretical Physics, University of Heidelberg, Philosophenweg 16, D-69120 Heidelberg, Germany

E-mail: sara.jamali@mail.um.ac.ir, mroshan@um.ac.ir,
l.amendola@thphys.uni-heidelberg.de

Abstract. We investigate the cosmological perturbations in the context of a Scalar-Tensor-Vector theory of Gravity known as MOG in the literature. Although MOG is plagued by ghosts, it does not suffer from tachyonic instability. Therefore it can be considered as a valid theory, at least in the classical limit. In the weak field limit, MOG increases the strength of gravity, and consequently addresses some astrophysical tests, without invoking dark matter particles. Recent investigations show that MOG reproduces a viable background cosmological evolution comparable to Λ CDM. However, the matter dominated era is slightly faster in MOG compared to Λ CDM. In this paper, in order to clarify whether this evolution is compatible with observations, we study the linear matter perturbations and estimate the relevant modified gravity parameters. In contrast to some current claims in the relevant literature, we show that MOG reduces the growth rate of the perturbations. We then compare MOG to the redshift space distortion (RSD) data. We find that MOG yields a much higher value than Λ CDM for the power spectrum parameter σ_8 . Although MOG cannot yet be ruled out by RSD data alone, the low growth and high σ_8 constitute a powerful challenge to the cosmological viability of MOG.

Contents

1	Introduction	1
2	The Scalar-Tensor-Vector theory	3
3	The perturbed equations	5
4	Perturbations in the sub-horizon scale	7
5	Numerical integration	13
6	Comparison with observation	17
7	Discussion and Conclusion	19
A	Appendix	20

1 Introduction

The Scalar-Vector-Tensor theory of gravity, also known as MOG in the literature, has been introduced in [1]. MOG does not includes dark matter but introduces instead two scalar fields, G and μ , and one vector field, ϕ_α , in addition to the metric tensor. The existence of three extra fields provides some degrees of freedom through which MOG addresses the dark matter problem. It is worth mentioning from the start that MOG is plagued by ghosts, as can be seen by wrong signs of the kinetic terms in the action (see (2.3) below). However, this theory does not suffer from the tachyonic instability. This means that, at least in the non-quantum limit suitable for the cosmological implications, MOG can be considered as a viable theory. For a detailed discussion on this aspect of MOG, see [2].

It is well-known that cold dark matter is needed to explain observations at different scales and in different systems, from spiral galaxies, to galaxy clusters, to the cosmological context. On the other hand, in a modified gravity model in which dark matter is absent, observations are explained by a suitable modification of the gravitational law. The astrophysical consequences of MOG have been widely investigated in, for example, [3]-[10]. In [3], it has been shown that MOG can explain the flat rotation curve of spiral galaxies with universal values for MOG's free parameters α and μ_0 (see below), which are related to the background values of the scalar fields G and μ . Moreover, applying a similar procedure to Chandra X-ray Telescope data, it is shown in [4] that MOG can also explain the mass discrepancy in galaxy clusters. Finally, the absence of dark matter particles in MOG leads to less dynamical friction experienced by baryonic matter in spiral galaxies and, consequently, faster stellar bars for spiral galaxies compared with the standard case (for more details see [9]).

It is natural to expect deviations from GR also in the strong field limit. MOG black holes have been widely investigated in the literature, for example see [13]-[17]. While MOG is consistent with the recently discovered gravitational wave signals [12], it has been shown in [11] that the quasinormal modes of gravitational perturbations in the ringdown phase of the merging of two MOG black holes have different frequencies compared to those of GR. This difference can be discriminated in future gravitational wave observations. To the best of our

knowledge, there are currently no theoretical or observational evidence implying the failure of MOG in the strong field limit.

In this paper, we focus on the cosmological behavior of the theory, in particular on the evolution of linear perturbations. Using the dynamical system analysis, the exact behavior of the MOG extra fields in the cosmic history of the universe has been investigated in [18]. The cosmic evolution starts from a standard radiation dominated era, evolves towards a matter dominated epoch and tends to a late time accelerated phase. In [2], we investigated the cosmology of MOG at the background level and showed that the model cannot fit the observational data of the sound horizon angular size. However, a slightly different version of MOG, called mMOG, gives a good agreement with the sound horizon data, although the matter dominated era of mMOG remains slightly different from Λ CDM.

It is claimed in the literature that MOG increases the growth rate of matter perturbations, compared to Λ CDM [19, 20]. Of course, this is the main feature that one might expect from a modified theory of gravity aiming at replacing dark matter particles, since a higher-than-standard growth rate is needed to compensate for the absence of dark matter. For an example of this point see [21]. This feature is reminiscent of what happens when we consider the rotation curves of spiral galaxies in the weak field limit, in which a stronger gravity replaces dark matter. Of course for theories that change the "dynamics" and not the gravitational sector, like the classic version of Modified-Newtonian-Dynamics (MOND), the above-mentioned feature does not apply.

However, most recent studies of linear perturbations in MOG impose some assumptions which restrict the validity of the results. For example, the authors of [19, 20] use the modified Poisson equation in MOG obtained in a non-expanding universe. Furthermore, they ignore the evolution of perturbations in some scalar fields: in [19], for example, the scalar field G is assumed to be constant.

In this paper we revisit the linear perturbations in MOG without any of these restrictive assumptions. As we will show, our results are significantly different from the precedent papers. More specifically, we do not confirm the main claim that MOG increases the growth rate of matter perturbations: we find rather a slower growth. Comparing to the available redshift space distortion (RSD) data, we find that to compensate the slower growth, the normalization σ_8 has to be substantially higher than in Λ CDM. Although *per se* this fact does not rule out MOG, such a high value will probably be in conflict with lensing and CMB results.

The perturbation equations we derive in this work can also be used to address CMB and lensing data. However, a full treatment of this requires a complete reanalysis of the data and we leave it to a future work. Concerning CMB, one could imagine that at early times MOG is corrected in some way to match CMB observations: in this case, only the late-time evolution studied in this paper will allow constraining or rule out the model.

This paper is organized as follow. In section 2 we briefly review the modified Friedmann equations. In section 3, we introduce the linear scalar perturbations in the metric, scalar and vector fields. We comprehensively investigate the perturbed field equations of the theory and we derive the perturbed field equations in an expanding universe. Then we proceed to find the evolution of matter perturbations, as a key issue to compare the model with observations. In section 4 we apply the sub-horizon limit to the perturbed equations, and find the final equation governing the evolution of baryonic perturbations in the matter dominated era in MOG. We follow the same procedure for linear perturbations in mMOG.

Using both analytical and numerical methods, we discuss the main features of the evolution of matter perturbations δ and growth rate function f . In section 6, applying the likelihood

analysis of the RSD data for $f\sigma_8$, we find the best value of σ_8^0 for MOG and mMOG. The results are reported and discussed in section 7.

2 The Scalar-Tensor-Vector theory

The action of Scalar-Tensor-Vector theory of Gravity, known also as MOG [22], is

$$S = S_{\text{gravity}} + S_{\text{scalar fields}} + S_{\text{vector field}} + S_m \quad (2.1)$$

in which,

$$S_{\text{gravity}} = \int \sqrt{-g} d^4x \left(\frac{R - 2\Lambda}{16\pi G} \right) \quad (2.2)$$

$$S_{\text{scalar fields}} = \int \sqrt{-g} d^4x \frac{1}{2G} g^{\mu\nu} \left(\frac{\nabla_\mu G \nabla_\nu G}{G^2} + \frac{\nabla_\mu \mu \nabla_\nu \mu}{\mu^2} \right) \quad (2.3)$$

$$S_{\text{vector field}} = \int \sqrt{-g} d^4x \frac{1}{4\pi} \left(\frac{1}{4} B_{\mu\nu} B^{\mu\nu} + V_\phi \right) \quad (2.4)$$

where R is the Ricci scalar, Λ is the effective cosmological constant and the anti-symmetric tensor $B_{\mu\nu}$ is written as $\nabla_\mu \phi_\nu - \nabla_\nu \phi_\mu$, where ϕ_μ is the vector field.

We recall that MOG has been introduced as an alternative theory of gravity for dark matter, not dark energy. The accelerated expansion in MOG is achieved as in GR, that is by adding a cosmological constant Λ . However, it should be noted that here Λ is slightly different from the cosmological constant in GR, since Λ in MOG appears as a mass term for the scalar field G . This can be inferred from action (2.2), where the term $V(G) = -\frac{\Lambda}{8\pi G}$ appears as a self interacting potential for G . For a more detailed description, we refer the reader to the equation (A.5) in [18].

The vector field potential V_ϕ is set to $-\frac{1}{2}\mu^2\phi_\alpha\phi^\alpha$, in which μ , in general, is a scalar field which plays the role of the mass of the vector field. This potential is the original form introduced in [1], that also leads to a viable weak field limit and also to an acceptable sequence of cosmic epochs. The action of matter, $S_m(g_{\alpha\beta}, \phi_\alpha)$, is postulated to be coupled to the vector field. In this case, there will be a non-zero fifth force current J_α . For the sake of simplicity and without loss of generality, we restrict ourselves to the case in which the scalar field μ is constant during the structure formation era. It should be mentioned that this scalar field does not play a crucial role in the cosmic history of MOG [23, 24]. More specifically it is shown in [2] and [18] that μ does not carry a substantial contribution to the total energy budget. In contrast, the scalar field G seriously influences the dynamics of the gravitating systems [3, 4].

It is useful to mention that, without μ , ϕ^α and Λ , MOG reduces to the Brans-Dicke scalar-tensor theory in its original form [25] with the dimensionless coupling constant $\omega_{BD} = -8\pi$. It is well known that in Brans-Dicke theory the coupling constant should be large, i.e., $\omega_{BD} \gg 1$, in order to pass the solar system observations. Therefore one may conclude that MOG cannot pass the classical tests in the absence of the vector field.

The energy-momentum tensors associated with the scalar field \mathcal{G} , defined as $\mathcal{G} = 1/G$, and with the vector field ϕ_α , are defined as follows

$$T_{\mu\nu}(\mathcal{G}) = -\frac{2}{\sqrt{-g}} \frac{\delta S_{\mathcal{G}}}{\delta g^{\mu\nu}} = -\frac{\nabla_\mu \mathcal{G} \nabla_\nu \mathcal{G}}{\mathcal{G}} + \frac{1}{2} g_{\mu\nu} \frac{\nabla_\alpha \mathcal{G} \nabla^\alpha \mathcal{G}}{2\mathcal{G}}, \quad (2.5)$$

$$T_{\mu\nu}(\phi_\alpha) = -\frac{2}{\sqrt{-g}} \frac{\delta S_\phi}{\delta g^{\mu\nu}} = -\frac{1}{4\pi} \left[B_\mu^\alpha B_{\nu\alpha} - g_{\mu\nu} \left(\frac{1}{4} B^{\rho\sigma} B_{\rho\sigma} + V_\phi \right) + 2 \frac{\partial V_\phi}{\partial g^{\mu\nu}} \right]. \quad (2.6)$$

Now let us briefly review the field equations of the theory. Variation of the action (2.1) with respect to $g^{\mu\nu}$, yields the following modified Einstein equation

$$G_{\mu\nu} - \frac{\nabla_\mu \nabla_\nu \mathcal{G}}{\mathcal{G}} + g_{\mu\nu} \frac{\square \mathcal{G}}{\mathcal{G}} + \Lambda \mathcal{G} g_{\mu\nu} = \frac{8\pi}{\mathcal{G}} (T_{\mu\nu(\mathcal{G})} + T_{\mu\nu(\phi_\alpha)} + T_{\mu\nu(m)}) \quad (2.7)$$

where $T_{\mu\nu(m)} = -\frac{2}{\sqrt{-g}} \frac{\delta S_m}{\delta g^{\mu\nu}}$ and $G_{\mu\nu}$ is the Einstein tensor. On the other hand, by varying the actions (2.3) and (2.4) with respect to \mathcal{G} and ϕ_α , the following field equations can be derived

$$\square \mathcal{G} = \frac{1}{16\pi} R \mathcal{G} + \frac{1}{2\mathcal{G}} \nabla_\alpha \mathcal{G} \nabla^\alpha \mathcal{G} - \frac{\Lambda \mathcal{G}}{8\pi} \quad (2.8)$$

$$\nabla_\beta B^{\beta\alpha} = 4\pi J^\alpha - \mu^2 \phi^\alpha \quad (2.9)$$

where the d'Alembertian operator $\square \mathcal{G}$ is defined as $\nabla_\alpha \nabla^\alpha \mathcal{G}$, and the fifth force current is obtained by varying the matter action with respect to the vector field as $J^\alpha = \frac{1}{\sqrt{-g}} \frac{\partial S_m}{\partial \phi^\alpha}$. Now, using (2.8) and (2.9), we can find the following continuity equations for \mathcal{G} and ϕ_α

$$\nabla_\mu T^\mu_{\nu(\phi_\alpha)} = B_{\alpha\nu} J^\alpha - \frac{1}{4\pi} \frac{\partial V_\phi}{\partial \phi_\alpha} B_{\nu\alpha} + \frac{1}{4\pi} \nabla_\nu V_\phi - \frac{1}{2\pi} \nabla^\mu \left(\frac{\partial V_\phi}{\partial g^{\mu\nu}} \right), \quad (2.10)$$

$$\nabla_\mu T^\mu_{\nu(\mathcal{G})} = -\frac{R}{16\pi} \nabla_\nu \mathcal{G} + \frac{\Lambda}{8\pi} \nabla_\nu \mathcal{G}. \quad (2.11)$$

We suppose that the matter content of the universe is a perfect fluid. In this case, by assuming the continuity relation $\nabla_\alpha J^\alpha = 0$ (or equivalently $\nabla_\alpha \phi^\alpha = 0$), one finds

$$\nabla_\alpha T^\alpha_{\nu(m)} = -B_{\alpha\nu} J^\alpha, \quad (2.12)$$

(see [26] for more details). The assumption of isotropy and homogeneity leads to $B_{\alpha\nu} = 0$ at the background level. Therefore, by using eq. (2.12), one recovers the normal continuity equation for the ordinary matter.

It is convenient now to rewrite the relevant background equations using the e -folding time $\tau = \ln a$ and $\mathcal{H} = H a$, the conformal Hubble function:

$$\frac{\mathcal{G}''}{\mathcal{G}} = -\frac{\mathcal{G}' \mathcal{H}'}{\mathcal{G} \mathcal{H}} + \frac{\mathcal{G}'^2}{2\mathcal{G}^2} - \frac{2\mathcal{G}'}{\mathcal{G}} - \frac{3\mathcal{H}'}{8\pi \mathcal{H}} - \frac{3}{8\pi} + \frac{e^{2\tau} \Lambda}{8\pi \mathcal{H}^2}, \quad (2.13)$$

$$J_{0\tau}(\tau) = \frac{\mu^2 \phi_{0\tau}}{4\pi} \quad (2.14)$$

$$\rho = (\mathcal{H}^2 e^{-2\tau}) \left(\frac{\mathcal{G}''}{2\mathcal{G}} + \frac{3\mathcal{G}'}{8\pi} + \frac{3\mathcal{G}}{8\pi} - \frac{\mathcal{G}\Lambda}{8\pi \mathcal{H}^2 e^{-2\tau}} - \frac{\mu^2 \phi_0^2}{8\pi} \right) \quad (2.15)$$

$$p = (\mathcal{H}^2 e^{-2\tau}) \left(-\frac{\mathcal{G}' \mathcal{H}'}{8\pi \mathcal{H}} + \frac{\mathcal{G}'^2}{2\mathcal{G}} - \frac{\mathcal{G}'}{8\pi} + \frac{\mathcal{G}\Lambda}{8\pi \mathcal{H}^2 e^{-2\tau}} - \frac{\mathcal{G}\mathcal{H}'}{4\pi \mathcal{H}} - \frac{\mathcal{G}''}{8\pi} - \frac{\mathcal{G}}{8\pi} - \frac{\mu^2 \phi_0^2}{8\pi} \right) \quad (2.16)$$

where a prime stands for derivative with respect to τ . As we shall see, equations (2.13) and (2.14) are necessary to simplify the first order equations. In the Appendix A, we have reviewed some relevant results from [2] about the MOG background evolution.

We have now the full set of MOG equations. In the following section, we linearize them and investigate the growth of density perturbations, in particular near the present epoch.

3 The perturbed equations

Let us start with the following perturbed flat-space metric in the Newtonian gauge

$$ds^2 = e^{2\tau} \left[- (1 + 2\Psi) \mathcal{H}^{-2} d\tau^2 + (1 + 2\Phi) \delta_{ij} dx^i dx^j \right] \quad (3.1)$$

We work from now on in Fourier space, with \mathbf{k} denoting the wavevector. One can write the perturbed fields \mathcal{G} and ϕ_α as

$$\begin{aligned} \mathcal{G}(\tau) &= \mathcal{G}_0(\tau) + \mathcal{G}_1(\tau) e^{i\mathbf{k}\cdot\mathbf{r}} \\ \phi_\alpha &= (\phi_\tau, \phi_{\mathbf{i}}) = (\phi_{0\tau}(\tau) + \phi_{1\tau}(\tau) e^{i\mathbf{k}\cdot\mathbf{r}}, ik\phi_{1i}(\tau) e^{i\mathbf{k}\cdot\mathbf{r}}) \end{aligned} \quad (3.2)$$

where the subscript \mathbf{i} stands for any of three spatial components, i.e. (x, y, z) , and both background and perturbed quantities are functions of τ . From now on, the subscripts 0 and 1 specify the background and the first order perturbed fields, respectively.

We perturb now the energy-momentum tensors. Let us start with the energy-momentum tensor of the ordinary matter. In this case it is straightforward to show that

$$\begin{aligned} T_{0(m)}^0 &= -\left(\rho + \delta \rho e^{i\mathbf{k}\cdot\mathbf{r}}\right) \\ T_{0(m)}^i &= \frac{i}{\sqrt{3}k} \rho \theta (\omega + 1) e^{i\mathbf{k}\cdot\mathbf{r}} \\ T_{i(m)}^j &= (\rho \omega + c_s^2 \delta \rho e^{i\mathbf{k}\cdot\mathbf{r}}) + \Sigma_i^j \end{aligned} \quad (3.3)$$

where ω is the equation of state parameter, $\delta = \frac{\delta\rho}{\rho}$ is the density contrast, ρ is the background density, $\theta = i\mathbf{k}\cdot\mathbf{v}/\mathcal{H}$ is the velocity divergence and \mathbf{v} is the peculiar velocity. Perturbations in the fluid pressure p is given by $\delta p = c_s^2 \delta \rho$, where c_s^2 is the adiabatic sound speed of the fluid. Since matter is supposed to be approximated by a perfect fluid, we ignore the anisotropic stress tensor Σ_i^j .

Similarly, in the following we linearize the energy-momentum tensors associated with the fields \mathcal{G} and ϕ_α . To do so, we use equation (2.5), and find the first order perturbation of $T_{(\mathcal{G})}^{\mu\nu}$ shown as $\delta T_{(\mathcal{G})}^{\mu\nu}$. The result is

$$\begin{aligned} \delta T_{0(\mathcal{G})}^0 &= -\delta T_{i(\mathcal{G})}^i = \frac{\mathcal{H}^2 \mathcal{G}'_0}{2\mathcal{G}_0^2} \left(2\mathcal{G}_0 (\mathcal{G}'_1 - \Psi \mathcal{G}'_0) - \mathcal{G}_1 \mathcal{G}'_0 \right) e^{-2\tau+i\mathbf{k}\cdot\mathbf{r}}, \\ \delta T_{0(\mathcal{G})}^i &= -\frac{ik\mathcal{G}_1 \mathcal{G}'_0}{\sqrt{3}\mathcal{G}_0} e^{-2\tau+i\mathbf{k}\cdot\mathbf{r}} \end{aligned} \quad (3.4)$$

In a similar way, for the vector field ϕ_α , using equation (2.6), we have

$$\begin{aligned} \delta T_{0(\phi_\alpha)}^0 &= -\delta T_{i(\phi_\alpha)}^i = \frac{\mu^2 \mathcal{H}^2 \phi_{0\tau}}{4\pi} \left(\phi_{1\tau} - \phi_{0\tau} \Psi \right) e^{-2\tau+i\mathbf{k}\cdot\mathbf{r}}, \\ \delta T_{0(\phi_\alpha)}^i &= \frac{ik}{4\pi} \mu^2 \phi_{1i} \phi_{0\tau} e^{-2\tau+i\mathbf{k}\cdot\mathbf{r}} \end{aligned} \quad (3.5)$$

Now we find the linearized form of the conservation equations (2.10) and (2.11). To do so, we first start with the scalar field \mathcal{G} and use equations (2.11) and (2.5) to find the following

first order relations. In this case the covariant derivative of (2.5) at the perturbed level gives

$$\begin{aligned} \nabla_\mu \delta T_0^\mu_{(\mathcal{G})} &= \mathcal{G}_1'' \frac{(\mathcal{H}^2 \mathcal{G}_0')}{\mathcal{G}_0} + \mathcal{G}_1' \left(\frac{4\mathcal{H}^2 \mathcal{G}_0'}{\mathcal{G}_0} - \frac{3\mathcal{H}^2 (\mathcal{G}_0')^2}{2\mathcal{G}_0^2} + \frac{\mathcal{H}^2 \mathcal{G}_0''}{\mathcal{G}_0} + \frac{2\mathcal{H} \mathcal{G}_0' H'}{\mathcal{G}_0} \right) \\ &+ (\mathcal{G}_0')^2 \left(\frac{3\mathcal{H}^2 \Phi'}{\mathcal{G}_0} - \frac{\mathcal{H}^2 \Psi'}{\mathcal{G}_0} \right) + \Psi \left(-\frac{2\mathcal{H}^2 \mathcal{G}_0' \mathcal{G}_0''}{\mathcal{G}_0} + \frac{\mathcal{H}^2 (\mathcal{G}_0')^3}{\mathcal{G}_0^2} - \frac{4\mathcal{H}^2 (\mathcal{G}_1')^2}{\mathcal{G}} - \frac{2\mathcal{H} (\mathcal{G}_0')^2 \mathcal{H}'}{\mathcal{G}_0} \right) \\ &+ \mathcal{G}_1 \left(-\frac{\mathcal{H}^2 \mathcal{G}_0' \mathcal{G}_0''}{\mathcal{G}_0^2} + \frac{\mathcal{H}^2 (\mathcal{G}_0')^3}{\mathcal{G}_0^3} - \frac{2\mathcal{H}^2 (\mathcal{G}_0')^2}{\mathcal{G}_0^2} - \frac{\mathcal{H} (\mathcal{G}_1')^2 \mathcal{H}'}{\mathcal{G}_0^2} + \frac{k^2 \mathcal{G}_0'}{\mathcal{G}_0} \right), \\ \nabla_\mu \delta T_i^\mu_{(\mathcal{G})} &= \frac{ik \mathcal{G}_1 \mathcal{H}}{2\sqrt{3} \mathcal{G}_0^2} (2\mathcal{G}_0 (\mathcal{G}_0' \mathcal{H}' + \mathcal{H} (\mathcal{G}_0'' + 2\mathcal{G}_0')) - \mathcal{H} \mathcal{G}_0')^2 e^{-2\tau + i\mathbf{k} \cdot \mathbf{r}}, \end{aligned} \quad (3.6)$$

The temporal and spatial components of the right-hand side of (2.11) can be written as

$$\begin{aligned} \left(\frac{1}{16\pi} (R - 2\Lambda) \nabla_0 \mathcal{G} \right)_1 &= -\frac{e^{-2\tau + i\mathbf{k} \cdot \mathbf{r}}}{8\pi} (3\mathcal{H} \mathcal{H}' (\mathcal{G}_1' + \mathcal{G}_0' (\Phi' - 2\Psi)) + k^2 \mathcal{G}_0' (2\Phi + \Psi) - \mathcal{G}_1' e^{2\tau} \Lambda \\ &+ 3\mathcal{H}^2 (\mathcal{G}_1' + \mathcal{G}_0' (\Phi'' + 3\Phi' - \Psi' - 2\Psi))) \\ \left(\frac{1}{16\pi} (R - 2\Lambda) \nabla_i \mathcal{G} \right)_1 &= -\frac{ik \mathcal{G}_1}{8\pi \sqrt{3}} (3\mathcal{H} \mathcal{H}' + 3\mathcal{H}^2 - e^{2\tau} \Lambda) e^{-2\tau + i\mathbf{k} \cdot \mathbf{r}} \end{aligned} \quad (3.7)$$

By equating the right-hand side of equations (3.6) and (3.7), we see that the spatial component gives rise to a trivial relation. Notice that to show this one needs to insert the background equation for \mathcal{G}_0'' given in (2.13). On the other hand, the time component leads to a second-order differential equation for \mathcal{G}_1 , see equation (4.24). We will discuss this relation in the next section.

Now we return to the vector field's conservation equation (2.10). Let us first use equation (3.5) and linearize the left hand side of equation (2.10). The result is

$$\begin{aligned} \nabla_\mu \delta T_0^\mu(\phi_\alpha) &= 0 \\ \nabla_\mu \delta T_i^\mu(\phi_\alpha) &= -\frac{ik \mu^2 \mathcal{H}^2}{12\pi} \phi_{0\tau} (\sqrt{3} \phi_{1\tau} - 3\phi'_{1i}) e^{-2\tau + i\mathbf{k} \cdot \mathbf{r}} \end{aligned} \quad (3.8)$$

By keeping the first order terms on the right-hand side of (2.10), one can easily show that the time component vanishes. For the spatial components, it turns out that only the first term on the right-hand side contributes. Therefore the spatial component on the right hand side of (2.10) in the linear limit is written as

$$(B_{\alpha i} J^\alpha)_1 = -\frac{1}{3} ik \mathcal{H}^2 J_{0\tau} (\sqrt{3} \phi_{1\tau} - 3\phi'_{1i}) e^{-2\tau + ikr} \quad (3.9)$$

Equating now eqs. (3.8) and (3.9), and summing over the index i , one may easily find the following scalar equation

$$ik \mathcal{H}^2 e^{-2\tau + i\mathbf{k} \cdot \mathbf{r}} (4\pi J_{0\tau} - \mu^2 \phi_{0\tau}) (\sqrt{3} \phi_{1\tau} - A'_1) = 0 \quad (3.10)$$

where A_1 is $\sum_i \phi_{1i}$ and accordingly $A'_1 = \sum_i \phi'_{1i}$. However, by using the vector field equation (2.9), one can readily conclude that the first parenthesis of (3.10) vanishes, see equation (2.14). Moreover, by using the field equation of ϕ_α , we show now that the second parentheses is also zero. Let us first take the divergence of (2.9) by keeping in mind that $\nabla_\alpha \phi^\alpha = 0$ and

$\nabla_\alpha J^\alpha = 0$. Consequently we arrive at a constraint identity on $B_{\alpha\beta}$, namely $\nabla_\alpha \nabla_\beta B^{\alpha\beta} = 0$. By linearizing this constraint we find

$$(\mathcal{H}^5 - \mathcal{H})(f') + (6e^{2\tau}\mathcal{H}^3 - 4\mathcal{H}^4\mathcal{H}' - e^{2\tau}\mathcal{H}^2\mathcal{H}' - \mathcal{H}' + 4\mathcal{H}^5)f = 0 \quad (3.11)$$

where the function f is defined as $f = \sqrt{3}\phi_{1\tau} - A'_1$. One may straightforwardly conclude that $f = 0$. On the other hand, spatial isotropy implies that $A = \phi_{1x} + \phi_{1y} + \phi_{1z} = 3\phi_{1j}$, where $j = 1, 2, 3$. This directly yields a simple differential equation between vector field components as

$$\phi'_{1j} = \frac{\phi_{1\tau}}{\sqrt{3}} \quad (3.12)$$

which is equivalent to $A'_1 = \sqrt{3}\phi_{1\tau}$ and consequently we have $\nabla_\mu \delta T_{\nu}^{\mu} \Big|_{(\phi_\alpha)} = 0$, or equivalently $(B_{\alpha\nu} J^\alpha)_1 = 0$. This result has an interesting consequence. In fact, as we have already mentioned, the ordinary matter energy-momentum tensor, in principle, is not conserved in MOG. However, at the cosmological background level, this tensor is conserved because of the isotropy and homogeneity of the cosmic fluid. In this case, the following standard conservation equation holds in MOG

$$\rho' + 3(1 + \omega)\rho = 0, \quad (3.13)$$

where ω is the equation of state parameter. One might expect this conservation to break down when dealing with first order perturbations. However the calculations discussed above show that $T_{(m)}^{\mu\nu}$ is conserved even in the linearized limit, i.e. $\nabla_\mu \delta T_{\nu}^{\mu} \Big|_{(m)} = 0$, see equation (2.12). This conservation equation along with the relation (3.3) leads to the following expressions

$$\delta k^2 c_s^2 + \mathcal{H}^2(\omega + 1)\theta' + \theta\mathcal{H}((\omega + 1)(\mathcal{H}(3\omega - 1) - \mathcal{H}') - \mathcal{H}\omega') - k^2\Psi(\omega + 1) = 0 \quad (3.14)$$

$$3\delta c_s^2 + \delta' + \theta + 3\Phi' - 3\delta w + \theta w + 3w\Phi' = 0 \quad (3.15)$$

where (3.14) is obtained from the spatial component $\nabla_\mu \delta T_{i(m)}^{\mu} = 0$, and (3.15) is the corresponding time component.

Let us now summarize this section by considering the number of unknowns and equations. There are seven unknown perturbation quantities: $G_1, \phi_{1\tau}, \phi_{1i}, \rho, \theta, \Psi$ and Φ . Accordingly, we need seven equations to describe the evolution of the perturbed quantities. Three equations are given by the conservation equations. More specifically, the conservation equation of $T_{(G)}^{\mu\nu}$, i.e. equation (2.11) yields a differential equation for G_1 , see equation (4.24) in the next section, while the conservation equation for $T_{(m)}^{\mu\nu}$ gives the two differential equations (3.14) and (3.15). Moreover, using the identity $\nabla_\alpha \nabla_\beta B^{\alpha\beta} = 0$, we found a relation between the components of the vector field, see equation (3.12). Consequently, we still need three equations to construct a complete set of equations. To find these three equations, in the next section we use the time component of the vector field equation (2.9), along with the off-diagonal and time components of the field equation (2.7).

4 Perturbations in the sub-horizon scale

In this section, we investigate the evolution of the density parameter δ in the sub-horizon scale. Specifically, the sub-horizon scale corresponds to the scale at which the physical wavelength

$2\pi a/k$ is much smaller than the Hubble radius $1/H$. In order to apply the sub-horizon limit to the perturbed equations, we introduce the dimensionless length parameter $\lambda = \mathcal{H}/k$ and perform the limit $\lambda \ll 1$, keeping only terms up to the lowest order. We restrict ourselves to the matter dominated epoch in MOG, where structure formation occurs. Therefore it is natural to expect that the equation of state parameter and the sound speed are zero, i.e. $\omega = 0$ and $c_s^2 = 0$.

Keeping these assumptions in mind, the off-diagonal component of (2.7), leads to the following relation

$$\Phi + \Psi = -\frac{\mathcal{G}_1}{\mathcal{G}_0} \quad (4.1)$$

Now, equation (3.15) can be written as

$$\delta' + 3(c_s^2 - \omega)\delta = -(\theta + 3\Phi')(\omega + 1) \quad (4.2)$$

On the other hand equation (3.14) gives

$$\theta' - \left(\frac{6\omega + 3\omega_t - 1}{2} - \frac{\omega'}{1+\omega} \right) \theta = \frac{1}{\lambda^2} \left(\frac{c_s^2 \delta}{1+\omega} + \Psi \right) \quad (4.3)$$

where we have conveniently defined the total equation of state parameter ω_t as follows

$$\frac{\mathcal{H}'}{\mathcal{H}} = 1 + \frac{H'}{H} = -\frac{1}{2} - \frac{3}{2}\omega_t. \quad (4.4)$$

Differentiating (4.2) with respect to $\tau = \ln a$, and combining with (4.3), we arrive at

$$\delta'' = \frac{1}{2}(3\omega_t - 1)(\delta' + 3\Phi') + \frac{1}{\lambda^2} \left(\frac{\mathcal{G}_1}{\mathcal{G}_0} + \Phi \right) - 3\Phi''. \quad (4.5)$$

As we already mentioned, in the sub-horizon limit, we ignore Φ'' and Φ' in comparison with $\frac{\Phi}{\lambda^2}$. In order to find a relation between Φ and \mathcal{G}_1 , we exploit the perturbed time component of equation (2.7), namely

$$\begin{aligned} \frac{\Phi}{\lambda^2} + \frac{\Lambda\Phi}{e^{-2\tau}\mathcal{H}^2} + \frac{1}{\mathcal{G}_0} \left(\mathcal{G}_1 \left(\frac{1}{2\lambda^2} + \frac{3}{2} - \frac{2\pi(\mathcal{G}_0')^2}{\mathcal{G}_0^2} + \frac{e^{2\tau}\Lambda}{2\mathcal{H}^2} \right) + \left(\frac{4\pi\mathcal{G}_0'}{\mathcal{G}_0} + \frac{3}{2} \right) \mathcal{G}_1' - \frac{4\pi\rho(\delta + 2\Psi)}{e^{-2\tau}\mathcal{H}^2} \right. \\ \left. - \mu^2\phi_{0\tau}\phi_{1\tau} \right) = 0. \end{aligned} \quad (4.6)$$

By applying the sub-horizon limit for \mathcal{G} , the equation (4.6) is simplified as

$$\frac{\Phi}{\lambda^2} + \frac{1}{\mathcal{G}_0} \left(\frac{\mathcal{G}_1}{2\lambda^2} - \frac{4\pi\rho\delta}{e^{-2\tau}\mathcal{H}^2} - \mu^2\phi_{0\tau}\phi_{1\tau} \right) = 0 \quad (4.7)$$

Now we need to find the last term, i.e., $\mu^2\phi_{0\tau}\phi_{1\tau}$, in terms of the other perturbations. In order to quantify this term, we perturb the vector field equation (2.9). However, although this might seem trivial, let us first show that the constraints on J_α and ϕ_α , i.e. $\nabla_\alpha\phi^\alpha = 0$ and $\nabla_\alpha J^\alpha = 0$, do not add new first order equations for the vector fields.

We start from the fifth force current J^α which is defined by

$$J^\alpha = \kappa\rho_m u^\alpha \quad (4.8)$$

where u^α is the four-velocity, and ρ_m is the matter density [24]. The metric (3.1) induces the following four velocity

$$u^\alpha = \frac{dx^\alpha}{ds} = \left(\frac{d\tau}{a(1+\Psi)\mathcal{H}^{-1}d\tau}, \frac{dx^i}{a\mathcal{H}^{-1}d\tau} \right) \approx \left(\frac{\mathcal{H}}{a}(1-\Psi), \frac{v^i}{a} \right) \quad (4.9)$$

In this way, the four-vector J^α takes the following form

$$J^\alpha = (J^0, J^i) = (e^{-\tau}\mathcal{H}\kappa\rho + \mathcal{H}\kappa\rho(\delta - \Psi)e^{-\tau+i\mathbf{k}\cdot\mathbf{r}}, -\frac{i\theta\mathcal{H}\kappa\rho}{\sqrt{3}k}e^{-\tau+i\mathbf{k}\cdot\mathbf{r}}) \quad (4.10)$$

where $\theta = \frac{i\mathbf{k}\cdot\mathbf{v}}{\mathcal{H}}$ and $\rho_m = \rho + \delta\rho e^{i\mathbf{k}\cdot\mathbf{r}}$. We then show that $\nabla_\alpha J^\alpha = 0$ does not impose new constraints to the linear perturbations. Strictly speaking, $\nabla_\alpha J^\alpha = 0$ at the background level recovers the usual continuity equation for matter,

$$e^{-\tau}\kappa\mathcal{H}(\rho' + 3\rho) = 0 \quad (4.11)$$

see also equation (3.13). Similarly, the linearized version of $\nabla_\alpha J^\alpha = 0$ gives

$$-e^{-\tau+i\mathbf{k}\cdot\mathbf{r}}\mathcal{H}\kappa\rho(\delta' + \theta + 3\Phi') = 0, \quad (4.12)$$

which recovers equation (4.2) for $\omega = c_s^2 = 0$. In fact, we were expecting this result since J^α is proportional to ρ_m and equations (4.11) and (4.12) are the continuity equations for matter at the background and perturbed level.

Now, we consider the field equation (2.9) at the linear level. One can substitute J^0 from equation (4.10) to rewrite equation (2.14) as

$$\phi_{0\tau} = \frac{4\pi\kappa\rho e^\tau}{\mathcal{H}\mu^2} \quad (4.13)$$

On the other hand, the time and spatial perturbed components of (2.9) can be written as

$$e^{i\mathbf{k}\cdot\mathbf{r}} \left(\sqrt{3}k^2 A'_1 - 24\pi\mathcal{H}^2\Psi J_{0\tau} + 12\pi\mathcal{H}^2 J_{1\tau} - 3\phi_{1\tau}(\mathcal{H}^2\mu^2 + k^2) + 6\mathcal{H}^2\mu^2\Psi\phi_{0\tau} \right) = 0 \quad (4.14)$$

$$-ik e^{-2\tau+i\mathbf{k}\cdot\mathbf{r}} \left(\mathcal{H}^2 A''_1 + \mathcal{H} A'_1 \mathcal{H}' - \sqrt{3}\mathcal{H}^2 \phi'_{1\tau} - \sqrt{3}\phi_{1\tau} \mathcal{H} \mathcal{H}' + 4\pi\mathcal{J} - \mu^2 A_1 \right) = 0 \quad (4.15)$$

where $\mathcal{J} = \sum_i J_{1i}$. After some simple algebraic manipulations, using equation (3.12) and its derivative together with equation (4.13), and by taking into account that J^α is defined in equation (4.10), one finds the following equations from the time and spatial components, respectively

$$-3\mathcal{H}e^{i\mathbf{k}\cdot\mathbf{r}}(\phi_{1\tau}\mathcal{H}\mu^2 - 4\pi\kappa\rho e^\tau(\delta + \Psi)) = 0 \quad (4.16)$$

$$ie^{-2\tau+i\mathbf{k}\cdot\mathbf{r}} \left(4\sqrt{3}\pi\theta\mathcal{H}\kappa\rho e^\tau - k^2\mu^2 A_1 \right) = 0 \quad (4.17)$$

which results in a simple relation for $\phi_{1\tau}$ and A_1 , respectively

$$\phi_{1\tau} = \frac{4\pi\kappa\rho e^\tau(\delta + \Psi)}{\mathcal{H}\mu^2}, \quad (4.18)$$

$$A_1 = \frac{4\sqrt{3}\pi\theta\mathcal{H}\kappa\rho e^\tau}{k^2\mu^2}. \quad (4.19)$$

It is also straightforward to show that $\nabla_\alpha \phi^\alpha = 0$ does not lead to a new constraint. In fact, in the unperturbed background, this constraint is written as

$$\phi'_{0\tau} = -\frac{4\pi J_{0\tau}(\mathcal{H}' + 2\mathcal{H})}{\mathcal{H}\mu^2} = -\frac{4\pi\kappa\rho e^\tau(\mathcal{H}' + 2\mathcal{H})}{\mathcal{H}^2\mu^2} \quad (4.20)$$

It can be simply verified that equation (4.20) is the time derivative of (4.13). On the other hand, the linearized form of $\nabla_\alpha \phi^\alpha = 0$ reads

$$\begin{aligned} \sqrt{3}k^2 A_1 \mu^2 - 24\pi\kappa\rho e^\tau \Psi (\mathcal{H}' + 2\mathcal{H}) + 3\mathcal{H} ((\mathcal{H}' + 2\mathcal{H}) \phi_{1\tau} + \mathcal{H} (\phi'_{1\tau} - 2\Psi\phi'_{0\tau})) \\ + 12\pi\mathcal{H}\kappa\rho e^\tau (3\Phi' - \Psi') = 0. \end{aligned} \quad (4.21)$$

Using equations (3.12), (4.13), (4.19) and (4.20), this equation takes the following simple form

$$12\pi\mathcal{H}\kappa\rho e^\tau (\delta' + \theta + 3\Phi') = 0 \quad (4.22)$$

which is equal to (4.12). Therefore we showed that $\nabla_\alpha \phi^\alpha = 0$ and equivalently $\nabla_\alpha J^\alpha = 0$ do not lead to additional first order equations.

Now, let us return to equation (4.7) in which one can replace $\mu^2\phi_{0\tau}\phi_{1\tau}$ using equations (4.13) and (4.18). We ignore the term including Ψ in comparison with $\frac{\Phi}{\lambda^2}$. Finally equation (4.7) takes the following form

$$\frac{\Phi}{\lambda^2} + \frac{1}{\mathcal{G}_0} \left(\frac{\mathcal{G}_1}{2\lambda^2} - \frac{4\pi\rho\delta}{e^{-2\tau}\mathcal{H}^2} - \left(\frac{4\pi\kappa\rho}{e^{-\tau}\mathcal{H}\mu} \right)^2 \delta \right) = 0 \quad (4.23)$$

In order to find the perturbed fields \mathcal{G}_1 , Φ and Ψ , we require another relation. Therefore, as already mentioned, we use the time component of the conservation equation of $T_{\mathcal{G}}^{\mu\nu}$, see (3.6) and (3.7). This equation is written as

$$\begin{aligned} \mathcal{G}_1'' + \mathcal{G}_1' \left(\frac{3}{2} - \frac{3\omega_t}{2} - \frac{\mathcal{G}_0'}{\mathcal{G}_0} \right) + \mathcal{G}_1 \left(\frac{3}{16\pi} + \frac{\mathcal{G}_0'^2}{2\mathcal{G}_0^2} - \frac{9\omega_t}{16\pi} + \frac{1}{\lambda^2} + \frac{e^{2\tau}\Lambda}{8\pi\mathcal{H}^2} \right) - \mathcal{G}_0'(\Psi' - 3\Phi') \\ + \frac{\mathcal{G}_0}{4\pi\lambda^2} \left(\Phi + \frac{\Psi}{2} \right) + \frac{\mathcal{G}_0}{16\pi} \left(15\Psi' - 9\omega_t\Phi' - 6\Psi' + 6\Psi'' + \frac{4\Lambda\Psi}{e^{-2\tau}\mathcal{H}^2} \right) = 0. \end{aligned} \quad (4.24)$$

In fact, we use this equation instead of the field equation of \mathcal{G} given by (2.8). Keeping the lowest order of λ , (4.24) takes the following simple form

$$\frac{\mathcal{G}_1}{\lambda^2} + \frac{\mathcal{G}_0}{8\pi\lambda^2}(\Psi + 2\Phi) = 0 \quad (4.25)$$

Now, we have equations (4.1), (4.23) and (4.25) for three unknowns \mathcal{G}_1 , Φ and Ψ . Some algebraic manipulations gives

$$\begin{aligned} \Psi &= -\frac{16\pi(4\pi-1)\lambda^2\rho(4\pi\kappa^2\rho + \mu^2)}{(16\pi-3)\mathcal{G}\mathcal{H}^2e^{-2\tau}\mu^2}\delta \\ \Phi &= \frac{8\pi(8\pi-1)\lambda^2\rho(4\pi\kappa^2\rho + \mu^2)}{(16\pi-3)\mathcal{G}\mathcal{H}^2e^{-2\tau}\mu^2}\delta \\ \mathcal{G}_1 &= -\frac{8\pi\lambda^2\rho(4\pi\kappa^2\rho + \mu^2)}{(16\pi-3)e^{-2\tau}\mathcal{H}^2\mu^2}\delta \end{aligned} \quad (4.26)$$

As an aside, one can immediately derive the anisotropic stress $\eta = -\Phi/\Psi$ as follows

$$\eta = \frac{8\pi - 1}{8\pi - 2} \approx 1.04 \quad (4.27)$$

This quantity, which is unity in the standard case, can be measured by combining weak lensing and galaxy clustering. Although present constraints on this parameter are still very weak, in [28] it has been shown that a Euclid-like survey can measure a constant η to within a few percent. This might then be an additional way to distinguish MOG from standard gravity.

From now on, we focus on the matter perturbation growth. In the context of MOG, the evolution of density contrast in the matter dominated era takes the form

$$\delta'' + \left(\frac{1}{2} - \frac{3\omega_t}{2}\right)\delta' - \frac{4\pi - 1}{16\pi - 3} \left(\frac{16\pi(4\pi\kappa^2\rho + \mu^2)}{\mathcal{G}_0\mathcal{H}^2\mu^2e^{-2\tau}}\right)\delta\rho = 0. \quad (4.28)$$

To simplify this equation, we first replace \mathcal{G}_0 by $1/G_0$, then ρ by $\frac{3\mathcal{H}^2e^{-2\tau}\Omega_m}{8\pi G_0}$ and the term $\mathcal{H}e^{-\tau}$ by H . Finally, we find

$$\delta'' + \left(\frac{1}{2} - \frac{3\omega_t}{2}\right)\delta' - \frac{(4\pi - 1)}{(16\pi - 3)} \left(\frac{6H^2\kappa^2\Omega_m}{G_0\mu^2} + 4\right) \frac{3}{2}\Omega_m\delta = 0. \quad (4.29)$$

The coefficient

$$Y \equiv \frac{(4\pi - 1)}{(16\pi - 3)} \left(\frac{6H^2\kappa^2\Omega_m}{G_0\mu^2} + 4\right) \quad (4.30)$$

represents the modification of the Poisson equation induced by MOG terms. One has $Y = 1$ in the standard gravity. This coefficient is variously denoted as G_{eff} or μ in current literature. Together with η given above, it fully characterizes the theory at linear, quasi-static scales.

If we ignore the vector field (this can be simply done by setting κ to zero), then equation (4.29) recovers the corresponding equation in Brans-Dicke theory with $\omega_{BD} = -8\pi$, see equation (11.164) in [27]. This is of course a consequence of the fact that in the absence of the vector field, MOG is equivalent to Brans-Dicke theory with $\omega_{BD} = -8\pi$.

In order to simplify equation (4.29), we use some results that are presented in Appendix A. Using the density parameters, i.e., equation (A.3), and considering the Table 2, it can be concluded that Ω_μ is almost negligible during the cosmic evolution. This result confirms our previous assumption that the scalar field μ can be assumed to be constant in our analysis. Furthermore, one can clearly see that the cosmological constant does not contribute to the energy budget of the matter dominated era. Now, using equation (A.2) we write

$$\frac{12H^2\kappa^2\Omega_m^2}{G_0\mu^2} = 1 - (\Omega_m + \Omega_R + \Omega_G + \Omega_\Lambda) \quad (4.31)$$

and combining equations (4.29) and (4.31), we arrive at

$$\delta'' + \left(\frac{1}{2} - \frac{3\omega_t}{2}\right)\delta' - \frac{3}{2}\Omega_m Y_{\text{MOG}}\delta = 0. \quad (4.32)$$

where now we see that

$$Y_{\text{MOG}} = \frac{(4\pi - 1)}{2\Omega_m(16\pi - 3)} \left(1 - \Omega_R - \Omega_G - \Omega_\Lambda + 7\Omega_m\right) \quad (4.33)$$

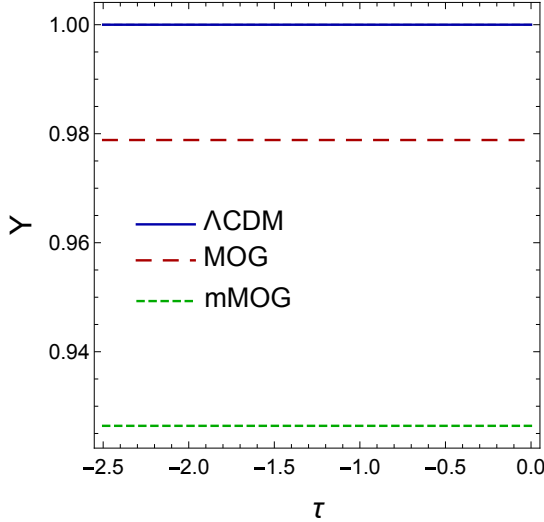


Figure 1. The evolution of the coefficients Y_{MOG} and Y_{mMOG} for $c = 0.33 \times 8\pi$ is compared to the ΛCDM case, i.e., the blue line $Y = 1$. The smaller Y for MOG and mMOG results in a slower growth rate.

This is the main expression needed to investigate the linear perturbations in MOG. Let us compare it with the corresponding equation in ΛCDM , namely

$$\delta'' + \left(\frac{1}{2} - \frac{3\omega_t}{2} \right) \delta' - \frac{3}{2} \Omega_m \delta = 0. \quad (4.34)$$

It is clear that the main difference between equations (4.32) and (4.34) is the coefficient Y , since ω_t evolves similarly in both MOG and ΛCDM , see Table 2 and 3 in the Appendix A. This coefficient can qualitatively specify whether the growth rate in MOG is lower or higher than that of ΛCDM . Using the numerical solutions reviewed in Appendix A, the evolution of Y is shown in Fig. 1, for MOG, mMOG and ΛCDM . The magnitude of Y in MOG and mMOG is smaller than ΛCDM . Therefore one may expect a slower growth rate for matter perturbations in MOG. This figure reveals another interesting feature, namely that Y in MOG and mMOG is also constant. One can easily verify that flat Y means that the left-hand side of (4.31) remains very small during the cosmic evolution. To be specific, let us write the left-hand side of equation (4.31) as follows

$$\xi \left(\frac{H}{H_0} \right)^2 \left(\frac{G_N}{G_0} \right)^2 \left(\frac{\mu_0}{\mu} \right)^2 \Omega_m^2 \quad (4.35)$$

where G_N is Newton's gravitational constant, μ_0 is the current value of the scalar field μ and ξ is a dimensionless parameter defined as

$$\xi = \frac{\kappa^2 H_0^2}{G_N \mu_0^2} = \frac{\alpha H_0^2}{\mu_0^2} \quad (4.36)$$

where $\alpha = \kappa^2/G_N$. This parameter and μ_0 are two well-known parameters in MOG and their observational values obtained from rotation curve data of spiral galaxies are $\alpha \simeq 8.89$

and $\mu_0 \simeq 0.042 \text{ kpc}^{-1}$ [3, 4]. Using these values along with the current value of the Hubble parameter, we find

$$\xi \simeq 5.6 \times 10^{-10} h^2 \quad (4.37)$$

This very small value for ξ is the main reason for Y to remain constant. Let us write this condition, i.e., $\xi \ll 1$, as follows

$$\lambda_\phi \ll d_H \quad (4.38)$$

where $\lambda_\phi = 1/\mu_0$ is the Compton wavelength of the vector field and d_H is the Hubble distance. In other words, the length scale of the field is negligible compared with the cosmological Hubble length. This fact directly means that the vector field is not light enough to play a significant role at cosmological scales. On the other hand, as we already mentioned, also the energy density of μ is sub-dominant during the cosmological expansion. Consequently, we can say that in MOG the only cosmologically important field is the scalar field G . In other terms, MOG is equivalent to a single scalar field Brans-Dicke theory. Unlike the screening fields, MOG's fields are hidden at cosmological scales where the density is low, and are important at high densities and smaller scales, like in galaxies and galaxy clusters.

To obtain another crude comparison between the growth rates in standard description and MOG, let us simply assume that Ω 's are almost constant in the matter dominated universe (this assumption is not too restrictive, especially when we look at the matter dominated phase as a fixed point in the dynamical system approach), and rewrite (4.32) as follows

$$\delta'' + k_1 \delta' - k_2 \delta = 0. \quad (4.39)$$

The growing solution is written as

$$\delta \propto a^{\frac{1}{2}(\sqrt{k_1^2 + 4k_2} - k_1)} \propto t^{\frac{\sqrt{k_1^2 + 4k_2} - k_1}{3(1 + \omega_t)}} \quad (4.40)$$

In the Newtonian case, where $\omega_t = 0$, we have $k_1 = 1/2$ and $k_2 = 3/2$ (if $\Omega_m = 1$ in matter dominated phase), and consequently $\delta \propto a \propto t^{2/3}$. It is required that modified gravity theories aiming at replacing dark matter should increase the growth rate of density contrast in baryonic matter compared with the standard case. Therefore, in MOG we expect that $\sqrt{k_1^2 + 4k_2} - k_1 > 2(1 + \omega_t)$, or equivalently

$$k_2 > (1 + \omega_t)^2 + (1 + \omega_t)k_1 \quad (4.41)$$

Using the matter dominated era values in Table 2, we find $k_1 = 0.52$ and $k_2 = 1.42$. Therefore one may simply conclude that the condition (4.41) does not hold in MOG. Our simple estimation shows then that although the scale factor grows close to the standard case, i.e. $a \propto t^{2/3}$, the matter contrast grows slower, as $\delta \propto t^{0.65}$, compared to the Newtonian case.

5 Numerical integration

Now, let us solve (4.32) in a completely general way. We need first to find a suitable set of initial conditions. We begin with the simplest choice, that is, the same initial conditions of Λ CDM in the deep matter dominated phase, namely

$$\delta'(\tau^*) = \delta(\tau^*), \quad \delta(\tau^*) = a^*. \quad (5.1)$$

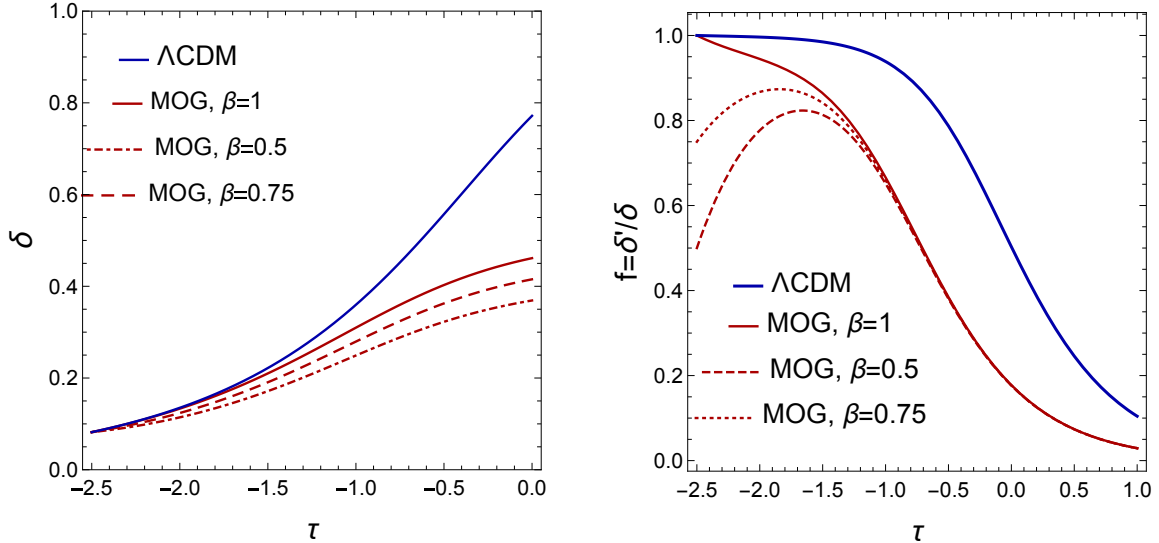


Figure 2. *Left panel:* The evolution of δ in MOG and Λ CDM. The initial conditions for Λ CDM and MOG is $\delta(-2.5) = 0.082$ and $\delta'(-2.5) = \delta(-2.5)$. *Right panel:* The growth rate function in MOG and Λ CDM with $f(-2.5) = 1$.

where the initial $\tau^* = \ln a^*$ is taken at $\tau = -2.5$, which corresponds to the redshift $z^* \simeq 11$. As advertised, and as we show in Fig. 2, we find that δ in MOG grows slower than in Λ CDM.

The initial conditions in modified theories of gravity, in principle, can be different from Λ CDM, for example see [29]. Consequently, we generalize the initial conditions as

$$\delta'(\tau^*) = \beta \delta(\tau^*) \quad (5.2)$$

where the new parameter, β , expresses the deviation from Λ CDM initial conditions. We need to consider only $\beta < 1$ since our analytic solution in the deep matter dominated epoch show that $\delta'/\delta = (\sqrt{k_1^2 + 4k_2} - k_1)/2 < 1$. As we show in the right panel in Fig. 2, we see that for any β the solution reverts soon back to the case $\beta = 1$. The conclusion that the growth of δ in MOG is slower than Λ CDM does not depend therefore on the initial conditions.

It is also instructive to investigate the growth rate f of matter perturbations, defined as follows

$$f = \frac{\delta'}{\delta} = \frac{d \ln \delta}{d \ln a} \quad (5.3)$$

Equation (4.32) can be written in terms of f as

$$f' + f^2 + \frac{1}{2}(1 - 3\omega_t)f - \frac{3}{2}\Omega_m Y_{\text{MOG}} = 0. \quad (5.4)$$

To solve this equation, we need only one initial condition, (5.2), namely $f(z^*) = \beta$. The result is illustrated in Fig. 2, right panel. This panel clearly confirms that the growth parameter f in MOG is always smaller than the standard case. It is interesting to mention that irrespective of the initial condition (β), the behavior of f does not change for $\tau > -1$. In fact if we perturb the initial condition, i.e. $\beta \rightarrow \beta + \delta\beta$, then the the growth rate will change as $f(\tau) \rightarrow f(\tau) + f_1(\tau)$, where $f_1(\tau)$ is a decreasing function of τ , as we show now through a simple first order stability analysis where $f_1 \ll f$. To do so, we use the functions $k_1(\tau)$ and $k_2(\tau)$ defined in (4.39), and linearize equation (5.4) as follows

$$f'_1 + (2f + k_1)f_1 = 0 \quad (5.5)$$

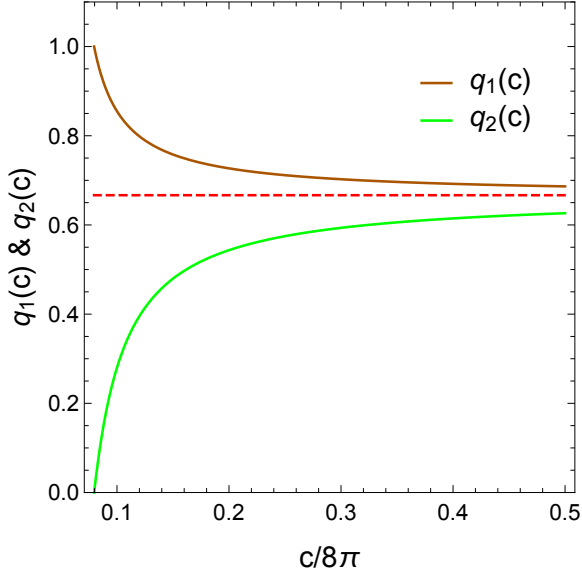


Figure 3. Evolution of q_1 and q_2 with respect to c where $a(t) \propto t^{q_1(c)}$ and $\delta \propto t^{q_2(c)}$. The curves smoothly reach the dashed green line which is the corresponding value for Λ CDM, i.e. $2/3$.

This equation can be simply integrated. The solution is

$$f_1 \propto e^{-\int^{\tau} (2f + k_1) d\tau}. \quad (5.6)$$

On the other hand we know that $f > 0$ and $k_1(\tau) > 0$. Therefore it is clear that f_1 is a decreasing function of τ , and the evolution of the growth rate parameter is independent of the initial condition. We will see that this behavior plays a key role to determine the observational parameter $f\sigma_8^0$ in MOG.

We now proceed to evaluate the growth rate in mMOG, a different version of MOG reviewed in the Appendix A. A new free parameter c has been incorporated by changing the kinetic energy contribution of the scalar field G . Following the same steps as for MOG, we find the following equation for the linear perturbation δ

$$\delta'' + \left(\frac{1}{2} - \frac{3\omega_t}{2} \right) \delta' - \frac{3}{2} Y_{\text{mMOG}} \Omega_m \delta = 0. \quad (5.7)$$

where

$$Y_{\text{mMOG}} = \frac{(c-2)}{(8c-12)\Omega_m} \left(1 - \Omega_R - \Omega_G - \Omega_\Lambda + 7\Omega_m \right) \quad (5.8)$$

where $\Omega_G = \frac{G'}{G} - \frac{c}{6} \left(\frac{G'}{G} \right)^2$ and the other Ω 's are the same as in equation (A.3). In order to avoid the existence of tachyonic instability, we restrict ourselves to positive c .

We first consider a crude approximation in which ω_t and Ω 's are constant. In this case, we are interested to see how δ in equation (5.7) is influenced by the new parameter c . We need to substitute the matter dominated fixed point's solution, see Table 3 in [2], into the equation (5.7). In this case it is straightforward to show that the cosmic scale factor grows as $a(t) \propto t^{q_1(c)}$, where the function $q_1(c)$ is as

$$q_1(c) = \frac{2(c-1)}{3c-4} \quad (5.9)$$

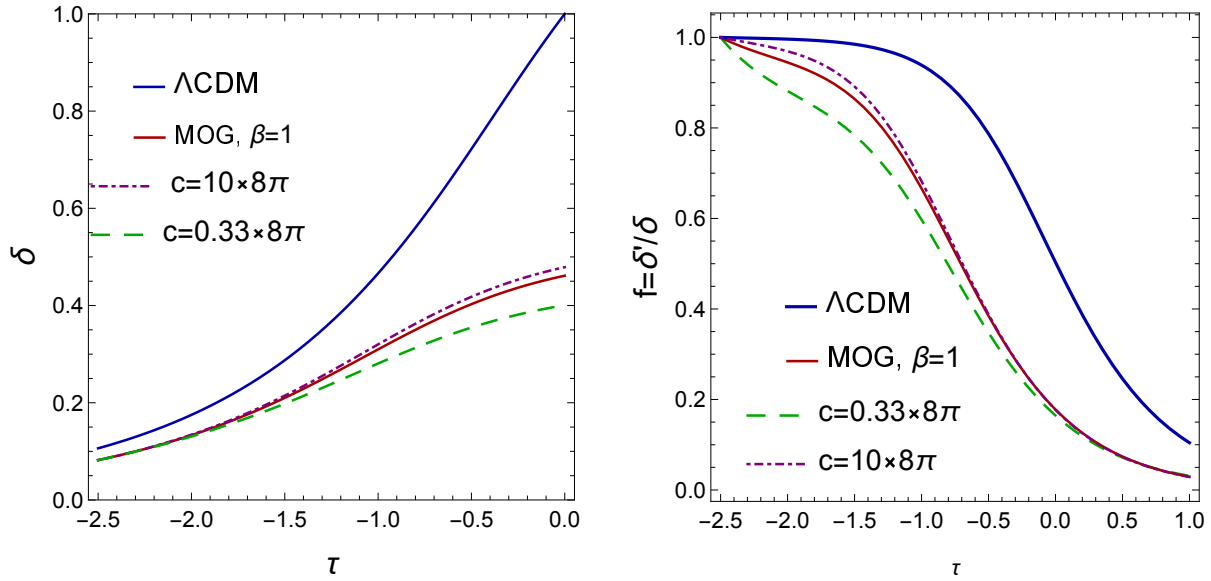


Figure 4. *Left panel:* The evolution of δ in mMOG for different choices of c . The initial conditions for Λ CDM and mMOG is $\delta'(-2.5) = \delta(-2.5)$ and $\delta(-2.5) = 0.082$. *Right panel:* The behavior of f in mMOG and Λ CDM. The growth of perturbations in mMOG is slower than Λ CDM, using the same initial condition, $f(-2.5) = 1$

With this solution, equation (5.7) is integrated to give $\delta \propto t^{q_2(c)}$ where

$$q_2(c) = \frac{\sqrt{50c^3 - 236c^2 + 370c - 192}}{2\sqrt{2c-3}(3c-4)} - \frac{c}{2(3c-4)} \quad (5.10)$$

It is clear that in the limit $c \rightarrow \infty$ both functions $q_{1,2}$ reach the standard value $2/3$.

In Fig. 3 we plot q_1 and q_2 in terms of the free parameter c . Since for $c < 2$ both functions are singular and negative we consider only $c > 2$. Fig. 3 reveals an interesting feature of the theory: irrespective of the magnitude of c , one has $q_1(c) > 2/3$ and $q_2(c) < 2/3$. This means that in mMOG the extra fields of the theory increase the expansion rate and decrease the growth of the matter perturbations for any viable value of c . Increasing the expansion rate, in principle, may reduce the matter growth. As an example, the Jeans analysis in a non-expanding isotropic and homogeneous fluid shows that matter perturbations grow exponentially with time while, in an expanding medium, they grow as a power law. For the special case $c = 0.33 \times 8\pi$ discussed in the Appendix A, we have $q_1 \simeq 0.7$ and $q_2 \simeq 0.6$. Therefore it seems that there is not a significant difference between MOG and mMOG as far as matter perturbations are concerned. This is confirmed by the exact numeric solution of (5.7) for the same initial conditions described for MOG. The result for different values of c is shown in Fig. 4, left panel. It is clear that the new parameter c does not lead to a significant deviation, although by decreasing c we need a larger value for δ at the initial time to recover the current matter perturbation, i.e. $\delta = 1$.

The corresponding growth rate parameter f is plotted in the right panel of Fig. 4. The solutions for different values of c are shown in the right panel of Fig. 4.

We can simply conclude that both MOG and mMOG lead to slower matter growth compared to Λ CDM. The reason is that the rate of growth depends heavily on the fraction of matter compared to other energy contributions. If the other homogeneous fields decrease this

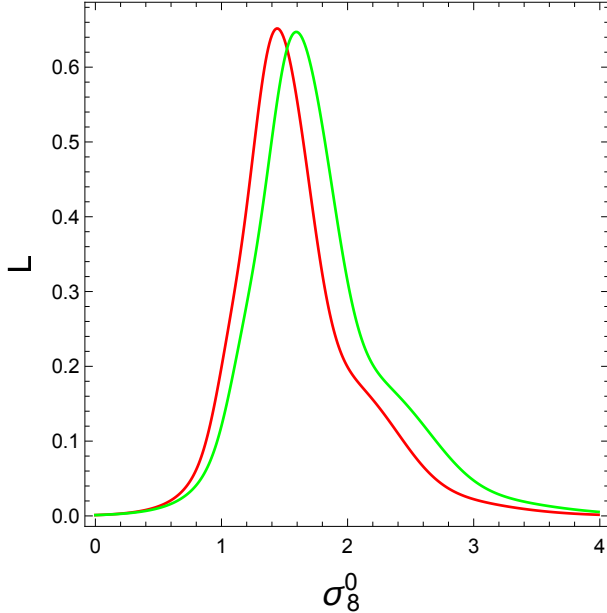


Figure 5. The likelihood function of σ_8^0 for MOG. The maximum values for MOG and mMOG correspond to $\sigma_8^0 = 1.44$ and 1.59 , respectively.

fraction, as it occurs here, the effect overcompensates the increase of gravitational strength, and the result is less growth.

In the following section, we compare our results with the relevant observation and discuss the viability of MOG as an alternative to dark matter particles.

6 Comparison with observation

In the previous section, we have obtained the evolution of the density perturbation δ and the growth function f in the context of MOG and a slightly modified version called mMOG. However, as we already mentioned, only the growth rate $f\sigma_8$, also called the RSD parameter, is actually observable, not the density contrast δ itself. Therefore here we use the available data for $f\sigma_8$ to compare (5.7) with observation. The RSD parameter $f\sigma_8$ is defined as

$$f\sigma_8 \equiv \sigma_8(z) \frac{\delta'(z)}{\delta(z)} \quad (6.1)$$

where

$$\sigma_8(z) = \sigma_8^0 \frac{\delta(z)}{\delta(0)}. \quad (6.2)$$

To obtain the current value of σ_8 , it is necessary to specify the underlying gravity theory. Then σ_8^0 is determined through model dependent observations such as CMB power spectrum [31], weak lensing [32] and abundance of clusters [33]. Consequently, σ_8^0 is a model-dependent quantity [34], and naturally one may expect a different value for it in MOG compared with Λ CDM (where $\sigma_8^0 = 0.802 \pm 0.018$ [31]), as we are going to find now.

We assume that $f\sigma_8(z)$ data are also valid in MOG¹. Then we solve the perturbation equation (5.7), and by fitting to $f\sigma_8(z)$ data, we predict the best value for σ_8^0 in MOG. It is worth mentioning that the available data for $f\sigma_8$ lie in the redshift range $0 \leq z \leq 1.2$ (see Fig. 6). In this interval, the baryonic matter, the cosmological constant and the scalar field G have non-zero contribution to the energy budget of the Universe, see Fig. 1 in [2]. On the other hand, one can ignore radiation in equation (5.7).

As we already discussed, equation (4.32) needs two initial conditions to be solved. Consequently, we have two free parameters σ_8^0 and β . However, we have already shown in the previous section that the evolution of perturbations does not change significantly with initial conditions, essentially because the growing mode dominates, regardless of the initial conditions. Therefore, without loss of generality, we set $\beta = 1$ as in Λ CDM.

For the data points, \mathcal{D}_i , we used Table II in [35]. In the case of independent data points, the likelihood function \mathcal{L} is given by a simple relation,

$$\mathcal{L} = A \exp[-\chi^2/2] \quad (6.3)$$

in which A is a normalization constant and χ^2 is defined as

$$\chi^2 = \sum_i \frac{(\mathcal{D}_i - \mathcal{T}_i)^2}{\sigma_i^2} \quad (6.4)$$

where \mathcal{D}_i and \mathcal{T}_i refer to the predicted value of an observable by data and theory, respectively. Furthermore, σ_i is the error associated with the i th data point. Specifically, in our case, we have

$$\mathcal{L} = \sum_i A \exp \left[-\frac{1}{2} \left(\frac{\mathcal{D}_i(z) - \sigma_8^0 \times \mathcal{T}_i(z)}{\sigma_i} \right)^2 \right]. \quad (6.5)$$

The results of the likelihood analysis for σ_8^0 are shown in Fig 5. The maximum of σ_8^0 is located at 1.44 and 1.59, for MOG and mMOG, respectively. Since in MOG matter is entirely constituted by the baryonic fraction, we anticipated a larger value for σ_8^0 , compared to Λ CDM, to compensate for the smaller matter gravitational pull. A similar situation can be seen in [36].

In Fig. 6, we plot $f\sigma_8$ for MOG, mMOG and Λ CDM along with the data points. We have shown the long-term evolution of $f\sigma_8$ for all the models, in the left panel of Fig. 6. We also fit a polynomial to the curves in MOG and mMOG. In the right panel, we restrict the plot to the available range of the data. In the case of Λ CDM we picked the reported σ_8^0 in [31], while for MOG and mMOG we used the result of our likelihood analysis. As the plot clearly shows, the evolution of $f\sigma_8$ in MOG and Λ CDM is significantly different. Although χ^2/dof is smaller in MOG, one needs more data points to decide which model can fit the data more accurately.

We summarize all the results obtained from the likelihood analysis in Table 1. The main conclusion is that both MOG and mMOG predict larger values for σ_8^0 . Of course, to make a reliable decision on the viability of MOG as an alternative theory of dark matter, it is necessary to measure σ_8^0 from other relevant observations, like CMB and lensing [37]. We leave this point to future studies. In TeVeS, a relativistic version for Modified Newtonian

¹It is necessary to mention that also $f\sigma_8$ is not completely model independent and in principle, one has to find it for the model under consideration. In the case of MOG, we can use the available data points, since MOG is designed to recover the same evolution for the background quantities as in Λ CDM

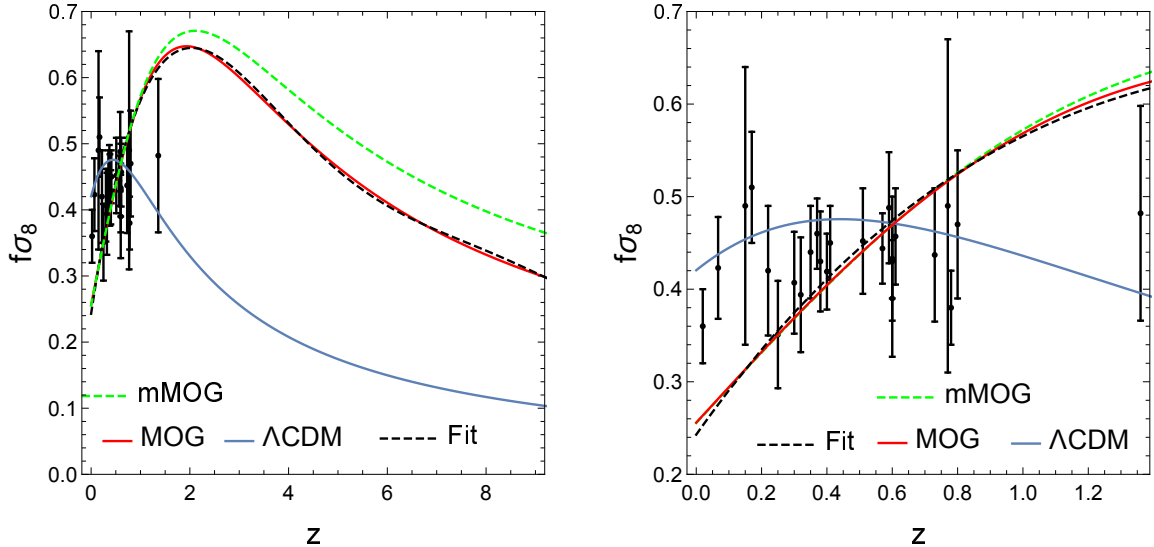


Figure 6. *Left panel:* The evolution of $f\sigma_8^0$ for ΛCDM , mMOG with $c = 0.33 \times 8\pi$, MOG and the best fit with the 5th order polynomial $\sum_k A_k a^k$, where $A_5 = 8 \times 10^{-5}$, $A_4 = -0.00275$, $A_3 = 0.03544$, $A_2 = -0.20970$, $A_1 = 0.49936$ and $A_0 = 0.24289$. *Right panel:* The same as the right panel but zoomed into a smaller range of redshift.

Dynamics (MOND) [38], the vector field can play a role similar to cold dark matter [21] and increase the matter growth rate. However, our analysis shows that this is not the case in MOG, and the Proca vector field does not expedite the perturbation growth. Therefore, our conclusion can be considered a challenge to the viability of this theory.

7 Discussion and Conclusion

In this paper, we investigated the cosmological perturbations in the context of a Scalar-Tensor-Vector theory of gravity known as MOG. As in the standard case, we started from the modified Friedmann equations and introduced the perturbed metric in the Newtonian gauge. We assumed that the matter content of the universe is a perfect fluid and, without imposing restrictive assumptions on the evolution of the fields, we found the first order perturbed field equations.

It is well known in the literature that any deviation from ΛCDM in matter dominated era may substantially influence the structure formation scenario. In order to consider this in detail, we evaluated the evolution of matter perturbations, δ , and the growth function, $f = \delta'/\delta$, in the context of MOG. Since the growth of gravitational seeds starts in the sub-horizon scale, we have considered the perturbed equations in the sub-horizon limit in the matter dominated epoch.

We also presented a similar description for mMOG, which is a different version of MOG compatible with the sound horizon observations. Our main result is that the growth of matter perturbations in both MOG and mMOG is slower than in ΛCDM . In fact, this is a surprising result, since in all the modified gravity theories aiming at replacing dark matter, the gravitational force should be strengthened in the weak field limit, in order to explain the flat galactic rotation curves, and other observations, without the pull of dark matter. However, we have shown that the reduced matter content of MOG overcompensates the extra gravitational force.

Λ CDM	MOG	mMOG
$\sigma_8^0 = 0.82$ [31]	$\sigma_8^0 = 1.44$	$\sigma_8^0 = 1.59$
$\chi^2/\text{dof} = 0.703$	$\chi^2/\text{dof} = 0.651$	$\chi^2/\text{dof} = 0.647$

Table 1. σ_8^0 and χ^2/dof for Λ CDM, MOG and mMOG.

We wrote down the full set of perturbation equations and determined the two modified gravity parameters, η and Y . We then compared MOG, mMOG and Λ CDM with the observed $f\sigma_8$, and found that MOG and mMOG require higher values for σ_8^0 . The RSD data do not yet rule out MOG but the high value of σ_8 seems problematic when compared to recent estimates due to lensing. Therefore we conclude that although MOG is not yet ruled out, a full analysis of CMB and lensing data will provide a strong challenge to MOG.

Acknowledgments

Sara Jamali thanks Henrik Nersisyan and Malihe Siavoshan for useful discussions. She also would like to thank the Institute for Theoretical Physics, University of Heidelberg for a very kind hospitality, during which some parts of this work have been done. Mahmood Roshan would like to thank Sohrab Rahvar for useful discussions.

A Appendix

In this appendix, we briefly review some results from [2] in which the cosmology of MOG has been investigated at the background level. Let us start with the familiar form of the flat FRW metric

$$ds^2 = -dt^2 + a(t)^2(dx^2 + dy^2 + dz^2). \quad (\text{A.1})$$

Using this metric and taking into account action (2.1), one of the modified Friedmann equations takes the following form

$$H^2 = \frac{8\pi G}{3}\rho + \frac{\Lambda}{3} + \frac{\dot{G}\dot{a}}{Ga} - \frac{4\pi}{3}(\frac{\dot{\mu}^2}{\mu^2} + \frac{\dot{G}^2}{G^2}) + \frac{1}{3}G\mu^2\phi_0^2. \quad (\text{A.2})$$

where $\rho = \rho_m + \rho_r$, ϕ_0 is the nonzero component of the vector field ϕ_α , and a dot denotes derivative with respect to cosmic time t . As we mentioned in the introduction section, it is clear from (A.2) that the kinetic terms of μ and G appear with the "wrong" sign. Although this means that this version of MOG have ghost, there is no tachyonic instability in this theory. Therefore MOG is viable, at least as long as a non-quantum treatment is sufficient. Using equation (A.2) one can define the following cosmic density parameters

$$\begin{aligned} \Omega_m &= \frac{8\pi G}{3H^2}\rho_m, & \Omega_r &= \frac{8\pi G}{3H^2}\rho_r, & \Omega_\Lambda &= \frac{\Lambda}{3H^2} \\ \Omega_G &= \frac{\dot{G}}{GH} - \frac{4\pi}{3}\left(\frac{\dot{G}}{GH}\right)^2, & \Omega_\mu &= -\frac{4\pi}{3}\left(\frac{\dot{\mu}}{\mu H}\right)^2. \end{aligned} \quad (\text{A.3})$$

Using a dynamical system analysis we find that, by setting appropriate initial conditions, MOG goes through a valid sequence of cosmological epochs (i.e., radiation, matter, acceleration), see Table 2. It is worth mentioning that MOG has other fixed points in which the

The epoch	$(\Omega_\Lambda, \Omega_m, \Omega_r, \Omega_G, \Omega_\mu)$	ω_{eff}	Stability
Radiation dominated	(0, 0, 1, 0, 0)	$\frac{1}{3}$	unstable
Matter dominated	(0, 0.97, 0, 0.03, 0)	-0.01	unstable
Dark energy dominated	(0.97, 0, 0, 0.03, 0)	-1	stable

Table 2. The cosmological epochs and their stability character for MOG, reproduced from [2].

The epoch	$(\Omega_\Lambda, \Omega_m, \Omega_r, \Omega_G, \Omega_\mu)$	ω_{eff}	Stability
Radiation dominated	(0, 0, 1, 0, 0)	$\frac{1}{3}$	unstable
Matter dominated	(0, 0.8, 0, 0.1, 0)	-0.05	unstable
Dark energy dominated	(0.9, 0, 0, 0.1, 0)	-1	stable

Table 3. The cosmological epochs and their stability for mMOG, reproduced from [2].

scalar fields G and μ are dominant, but for the reasons discussed in [2], they do not lead to an acceptable cosmology, and are then to be avoided by selecting appropriate initial conditions (notice that this is not a fine tuning, since there exist finite regions of initial conditions leading to the viable cosmology).

However, in [2] it was found that the predicted value of MOG for the sound horizon angular size is not compatible with the observed value. This fact led us to modify the kinetic term of the scalar field G and introduce mMOG (modified MOG), with the following action

$$S = \int \sqrt{-g} d^4x \left[\frac{(R-2\Lambda)}{16\pi G} + \frac{1}{4\pi} \left(\frac{1}{4} B_{\mu\nu} B^{\mu\nu} + V_\phi \right) + \frac{1}{2G} \left(\frac{c}{8\pi} \frac{\nabla_\mu G \nabla^\mu G}{G^2} + \frac{\nabla_\nu \mu \nabla^\nu \mu}{\mu^2} \right) \right]. \quad (\text{A.4})$$

with a new free parameter, c . The reason for this modification is that in the weak field limit of MOG, G has the role of strengthening gravity to address the dark matter problem [23]. Therefore, one may expect that a simple and effective modification of MOG consists in multiplying the kinetic term of G by a constant coefficient ². In order to avoid the tachyonic instability in the theory, c is expected to be positive and for $c = 8\pi$ we recover MOG. It turns out that mMOG with $c = 0.33 \times 8\pi$ brings the sound horizon angular size compatible with the observation, while at the same time achieving a viable sequence of cosmological epochs, see Table 3. Since both in MOG and mMOG the matter budget of the Universe is entirely baryonic, Ω_{m0} , the present value of the matter density parameter, is around 0.05, not 0.3 as in Λ CDM.

References

- [1] J. W. Moffat, JCAP 0603, 004 (2006).
- [2] S. Jamali, M. Roshan and L. Amendola, JCAP **1801**, no. 01, 048 (2018).
- [3] J. W. Moffat and S. Rahvar, Mon. Not. Roy. Astron. Soc. **441**, no. 4, 3724 (2014).

²Although one can also modify the kinetic term of μ , G plays the most important role in addressing the dark matter problem.

- [4] J. W. Moffat and S. Rahvar, *Mon. Not. Roy. Astron. Soc.* **436**, 1439 (2013).
- [5] N. Ghafourian and M. Roshan, *Mon. Not. Roy. Astron. Soc.* **468**, 4450 (2017).
- [6] J. R. Brownstein and J. W. Moffat, *Mon. Not. Roy. Astron. Soc.* **367**, 527 (2006).
- [7] M. Roshan, S. Abbassi and H. G. Khosroshahi, *Astrophys. J.* **832**, no. 2, 201 (2016).
- [8] M. Roshan and S. Abbassi, *Astrophys. J.* **802**, no. 1, 9 (2015).
- [9] M. Roshan, *Astrophys. J.* **854**, no. 1, 38 (2018).
- [10] N. S. Israel and J. W. Moffat, *Galaxies* **6**, no. 2, 41 (2018).
- [11] L. Manfredi, J. Mureika and J. Moffat, *Phys. Lett. B* **779**, 492 (2018).
- [12] M. A. Green, J. W. Moffat and V. T. Toth, *Phys. Lett. B* **780**, 300 (2018)
- [13] P. Sheoran, A. Herrera-Aguilar and U. Nucamendi, *Phys. Rev. D* **97**, no. 12, 124049 (2018)
- [14] J. R. Mureika, J. W. Moffat and M. Faizal, *Phys. Lett. B* **757**, 528 (2016)
- [15] J. W. Moffat, *Eur. Phys. J. C* **75**, no. 4, 175 (2015)
- [16] J. W. Moffat, *Eur. Phys. J. C* **75**, no. 3, 130 (2015)
- [17] F. G. Lopez Armengol and G. E. Romero, *Astrophys. Space Sci.* **362**, no. 11, 214 (2017)
- [18] S. Jamali and M. Roshan, *Eur. Phys. J. C* **76**, no. 9, 490 (2016).
- [19] F. Shojai, S. Cheraghchi and H. Bouzari Nezhad, *Phys. Lett. B* **770**, 43 (2017).
- [20] J. W. Moffat and V. T. Toth, *Galaxies* **1**, 65 (2013).
- [21] S. Dodelson and M. Liguori, *Phys. Rev. Lett.* **97**, 231301 (2006).
- [22] J. W. Moffat and V. T. Toth, *Class. Quant. Grav.* **26**, 085002 (2009).
- [23] J. W. Moffat, arXiv : 1409.0853.
- [24] J. W. Moffat, arXiv : 1510.07037.
- [25] C. Brans and R. H. Dicke, *Phys. Rev.* **124**, 925 (1961).
- [26] M. Roshan, *Phys. Rev. D* **87**, 044005 (2013).
- [27] L. Amendola and S. Tsujikawa, *Dark energy Theory and observation*, (Cambridge University Press, 2010)
- [28] L. Amendola, S. Fogli, A. Guarnizo, M. Kunz and A. Vollmer, *Phys. Rev. D* **89**, no. 6, 063538 (2014); A. M. Pinho, S. Casas and L. Amendola, *JCAP* **1811**, no. 11, 027 (2018).
- [29] C. Di Porto and L. Amendola, *Phys. Rev. D* **77**, 083508 (2008).
- [30] M. Roshan and S. Abbassi, *Phys. Rev. D* **90**, no. 4, 044010 (2014).
- [31] P. A. R. Ade *et al.* [Planck Collaboration], *Astron. Astrophys.* **594**, A13 (2016).
- [32] S. More, H. Miyatake, R. Mandelbaum, M. Takada, D. Spergel, J. Brownstein and D. P. Schneider, *Astrophys. J.* **806**, no. 1, 2 (2015).
- [33] P. A. R. Ade *et al.* [Planck Collaboration], *Astron. Astrophys.* **594**, A24 (2016).
- [34] H. Nersisyan, A. F. Cid and L. Amendola, *JCAP* **1704**, no. 04, 046 (2017).
- [35] I. Albarran, M. Bouhmadi-Lopez and J. Morais, *Phys. Dark Univ.* **16**, 94 (2017).
- [36] N. MacCrann, J. Zuntz, S. Bridle, B. Jain and M. R. Becker, *Mon. Not. Roy. Astron. Soc.* **451**, no. 3, 2877 (2015).
- [37] H. Hildebrandt *et al.*, *Mon. Not. Roy. Astron. Soc.* **465**, 1454 (2017)
- [38] J. D. Bekenstein, *Phys. Rev. D* **70**, 083509 (2004).